J Neurophysiol 89: 3114–3127, 2003.
First published February 26, 2003; 10.1152/jn.00014.2003.

PRQFVamide, a Novel Pentapeptide Identified From the CNS and Gut of *Aplysia*

Y. Furukawa,[1] K. Nakamaru,[1] K. Sasaki,[1] Y. Fujisawa,[3] H. Minakata,[3] S. Ohta,[2] F. Morishita,[1] O. Matsushima,[1] L. Li,[4] V. Alexeeva,[5] T. A. Ellis,[5] N. C. Dembrow,[5] J. Jing,[5] J. V. Sweedler,[4] K. R. Weiss,[5] and F. S. Vilim[5]

[1]*Graduate School of Science, Department of Biological Science and* [2]*Instrumental Center for Chemical Analysis, Hiroshima University, Higashi-Hiroshima 739-8526, Japan;* [3]*Suntory Institute for Bioorganic Research, Shimamoto, Mishima, Osaka 618-8503, Japan;* [4]*Department of Chemistry and Beckman Institute, University of Illinois, Urbana, Illinois 61801; and* [5]*Department of Physiology and Biophysics, Mount Sinai School of Medicine, New York, New York 10029*

Submitted 7 January 2003; accepted in final form 6 February 2003

Furukawa, Y., K. Nakamaru, K. Sasaki, Y. Fujisawa, H. Minakata, S. Ohta, F. Morishita, O. Matsushima, L. Li, V. Alexeeva, T. A. Ellis, N. C. Dembrow, J. Jing, J. V. Sweedler, K. R. Weiss, and F. S. Vilim. PRQFVamide, a novel pentapeptide identified from the CNS and gut of *Aplysia*. *J Neurophysiol* 89: 3114–3127, 2003. First published February 26, 2003; 10.1152/jn.00014.2003. We have purified a novel pentapeptide from the *Aplysia* nervous system using bioassay on gut contractions. The structure of the peptide is Pro-Arg-Gln-Phe-Val-amide (PRQFVa). The precursor for PRQFVa was found to code for 33 copies of PRQFVamide and four related pentapeptides. Peaks corresponding to the predicted masses of all five pentapeptides were detected in *Aplysia* neurons by matrix-assisted laser desorption/ionization time-of-flight mass spectrometry. Northern analysis revealed that expression of the precursor is abundant in the abdominal ganglion, much less in the pedal and cerebral ganglia, and rarely seen in the buccal and pleural ganglia. PRQFVa-positive neurons, mapped by immunohistochemistry and in situ hybridization, were present in all the central ganglia. PRQFVa immunopositive processes were observed in the gut, particularly in association with the vasculature. Some arteries and other highly vascularized tissues, such as the gill and the kidney, also contain numerous PRQFVa immunopositive processes. Application of synthetic PRQFVa suppresses not only contractions of the gut but also contractions of vasculature. PRQFVa is expressed in some of the neurons within the feeding circuitry and application of synthetic PRQFVa was found to decrease the excitability of some (B4/5 and B31/32) but not all (B8) neurons of the buccal feeding circuit. Our findings suggest that PRQFVa may act as a modulator within the feeding system as well as in other systems of *Aplysia*.

INTRODUCTION

Biogenic amines and amino acids are ubiquitous signaling molecules in the nervous system, and the same molecules are used for chemical transmission in most, if not all, animals across phyla. In addition to these small-molecule transmitters, animals use neuropeptides as intercellular signaling molecules (Strand 1999). The widespread presence and bioactivity of neuropeptides indicates that one must understand the role of neuropeptides as well as small-molecule transmitters to obtain a comprehensive understanding of the functioning of the nervous system. In the last 15 yr, motivated by different physiological and functional interests, several laboratories have identified a large number of bioactive peptides in different species. Furthermore, significant progress has been made toward understanding various functions of neuropeptides. The advantageous features of invertebrate nervous systems provide unique opportunities for investigators to study the role of neuropeptides, acting alone or as cotransmitters, within the nervous system both at the network and single-cell level (Brezina and Weiss 1997; Kupfermann 1991; Marder et al. 1995; Nusbaum et al. 2001).

One of the species in which neuropeptides have been extensively studied is the marine mollusk *Aplysia*. A number of laboratories have investigated the role of neuropeptides in feeding neuronal circuits and in peripheral tissues that implement feeding behavior. Within the CNS of *Aplysia*, neuropeptides have been shown to induce motor programs, alter the frequency of motor programs, and alter phase relationships of activity of different motor neurons within motor programs, thus producing motor program switching (Morgan et al. 2000, 2002; Sweedler et al. 2002). In the buccal mass, the feeding organ of *Aplysia*, neuropeptides alter excitation-contraction coupling, modify the relaxation rate of muscle contractions, and modify transmitter release from motor neurons (Brezina et al. 1996; Church et al. 1993; Cropper et al. 1987a,b; Lloyd et al. 1984). Neuropeptides also act within the gut, where some peptides induce and other peptides suppress gut motility (Fujisawa et al. 1999; Furukawa et al. 2001; Lloyd et al. 1988). However, even in this extensively studied preparation in which numerous neuropeptides have been identified, a number of observations made on neurons and nerves involved in feeding suggest that several as yet unidentified, potentially bioactive, peptides might be present in the system.

To further understand the feeding circuits and behaviors of *Aplysia*, we undertook a search for additional peptides that are present and bioactive in the feeding system of *Aplysia*. We purified a novel neuropeptide from CNS extracts using gut

Address for reprint requests: F. S. Vilim, Dept. of Physiology and Biophysics, Box 1218, Mount Sinai School of Medicine, New York, NY 10029 (E-mail: vilim@inka.mssm.edu).

The costs of publication of this article were defrayed in part by the payment of page charges. The article must therefore be hereby marked "*advertisement*" in accordance with 18 U.S.C. Section 1734 solely to indicate this fact.

contractions as a bioassay. We chose this bioassay because it is rapid and has been shown to be highly successful in isolating other peptides. This approach has successfully identified a number of neuropeptides also localized to ganglia that contain the neural circuit involved in generating feeding behavior (Fujisawa et al. 1999; Furukawa et al. 2001). In the present study, this approach has again proven successful. Using this approach, we now identify a novel neuropeptide, Pro-Arg-Gln-Phe-Val-amide (PRQFVa), and describe its purification, cloning, distribution, and some of its physiological effects.

METHODS

Animals

Two species of the opisthobranch mollusk *Aplysia* were used: *Aplysia kurodai* and *Aplysia californica*. Animals were kept in tanks filled with artificial seawater (ASW) continuously aerated at 14–15°C. *A. kurodai* (50–300 g) were caught in Hiroshima Bay and in Hamada City (the coast of the Sea of Japan) and transported to Hiroshima University on the same day. Some animals were provided from the marine biological station of Tohoku University (Asamushi, Japan). For peptide purification, animals were killed immediately after arrival. For physiological experiments, animals were kept in tanks filled with circulating filtered ASW at 15°C and fed with dried seaweed. Specimens of *A. californica* (10–500 g) were obtained from the *Aplysia* Research Facility (Miami, FL), Pacific Biomarine (Venice, CA), and Marinus (Long Beach, CA). Several larger animals (≤1000 g) were collected off the Monterey Peninsula between January and July 1998. Animals were used between 3 and 14 days of receipt. Large animals (200–500 g) were used for RNA extraction and MALDI MS, while both large and small (10–500 g) animals were used for immunocytochemistry (IMM) and in situ hybridization (ISH). Experiments were performed on different species of *Aplysia* because of differences in expertise of the groups involved and differential availability of *Aplysia* species in the United States and Japan.

Purification

The generation of extracts from the CNS of *A. kurodai*, as well as the methodology used for the purification of the pentapeptide reported in this study, was the same as that reported elsewhere (Furukawa et al. 2001). Briefly, the extract obtained by boiling CNS in 4% acetic acid was forced through C18 cartridge columns (Sep-pak C18; Waters, 12 ml, 2 g), and the retained material was eluted with 100% methanol/0.1% trifluoroacetic acid (TFA). The eluate was first fractionated by a reversed-phased column (Inertsil ODS-80A, 10 × 250 mm, GL Science) with a linear gradient of acetonitrile (0–100% in 200 min) containing 0.1% TFA. The activity of each 2-ml fraction was examined using a bioassay on the anterior gut of *A. kurodai*. Bioactive fractions were subjected to further purification step using a cation-exchange column (TSKgel SP-5PW; 7.5 × 75 mm, Tosoh, Tokyo, Japan) equilibrated with 10 mM sodium phosphate buffer, and the column was eluted with a linear gradient of NaCl (0–0.6 M in 120 min). Bioactive fractions that eluted at 0.19–0.21 M NaCl were further separated by a reversed-phase column (TSKgel ODS-80TM, 4.6 × 150 mm, Tosoh) with a linear gradient of acetonitrile (9–32% in 92 min) containing 0.1% TFA. The bioactive fraction that eluted at 13.8% acetonitrile was subjected to a final stage of purification on the reversed-phase column with isocratic elution using 13.8% acetonitrile/0.1% TFA, producing a single absorbance peak (220 nm). The structure of purified peptide was determined by sequencing, fast atom bombardment mass spectrometry (FAB-MS), and co-elution experiments as described previously (Furukawa et al. 2001).

Structural determination

Structural determination was performed as previously described (Fujisawa et al. 1999; Furukawa et al. 2001). Briefly, the purified peptides from *A. kurodai* were subjected to amino acid sequence analysis by an automated sequencer (PSQ-1, Shimadzu, Kyoto, Japan). For most peptides, to estimate a C-terminal structure, molecular masses were determined by FAB-MS, (SX-102A, JEOL, Tokyo, Japan). Based on the results, peptides having predicted structures were synthesized by a conventional solid-phase method by a peptide synthesizer (PSSM-8, Shimadzu) and purified by reverse-phase high-performance liquid chromatography (HPLC). To confirm their structure, retention times of synthetic and purified peptides were compared both on reverse-phase and cationic-exchange HPLC. When the information of molecular mass was not available, both C-terminally amidated and nonamidated peptides were synthesized, and their retention times in HPLC were compared with those of purified peptides.

Cloning

Cloning of the PRQFVa precursor from *A. californica* was performed using standard molecular techniques (Sambrook et al. 1989), except where noted. Semi-nested rapid amplification of cDNA ends (RACE) was performed on a Robocycler Gradient 40 (Stratagene, La Jolla, CA) with multiple annealing temperatures, as previously described (Fujisawa et al. 1999; Furukawa et al. 2001; Sweedler et al. 2002). An antisense degenerate oligo designed to PRQFVGKR (CK-YTTICCIACRAAYTGICKIGG, we assumed G as amide donor and a KR dibasic cleavage site to improve oligo annealing characteristics) was used with two bluescript vector primers (BS1 = ACCATGAT-TACGCCAAG and BS2 = AATTAACCCTCACTAAAG) on random primed *A. californica* ganglionic cDNA lambda library. Oligonucleotides were obtained from Operon (Alameda, CA) and used at a final concentration of 0.5–1 μM. The polymerase chain reaction (PCR) products were ligated into T/A cloning vector (Invitrogen, Carlsbad, CA) and sequenced using dye termination. Inserts from correct clones were used for library screening to identify additional cDNA clones and determine the coding sequence of the precursor. At least three independent clones were sequenced to obtain a consensus. Due to the highly repetitive nature of the PRQFVa precursor clone, exonuclease digestion was employed to generate deletions and facilitate sequence determination. Uni-Zap *A. californica* ganglionic cDNA libraries were a kind gift from G. Nagle (Marine Biomedical Institute, Galveston, TX), and the lambda Zap random primed *A. californica* cDNA library was a kind gift from Dr. Wayne Sossin (McGill University, Montreal, Canada).

Mass spectrometry

Mass spectrometry was performed on *A. californica* as previously described (Fujisawa et al. 1999; Furukawa et al. 2001; Sweedler et al. 2002). Briefly, ganglia with intact connectives and commissures were removed after an injection of 390 mM $MgCl_2$ equal to 50% of each animal's body weight. In some cases, a moderate protease treatment (e.g., 1% protease type IX for 30–60 min at 34°C) was used to soften the connective tissues prior to cell dissection. Extracellular salts were removed with washes of 10 mg/ml of 2,5-dihydroxybenzoic acid (DHB; ICN Pharmaceuticals, Costa Mesa, CA), and specific cells were identified and isolated based on the immunostaining results. Tungsten needles were used to isolate individual or group of cells onto a MALDI sample plate containing 0.5 μl of matrix solution. After drying at ambient temperature, samples were either frozen for future analysis or analyzed immediately.

Mass spectra were obtained using a Voyager DE-STR mass spectrometer equipped with delayed ion extraction (PE Biosystems, Framingham, MA). A pulsed nitrogen laser (337 nm) was used as the desorption/ionization source, and positive-ion mass spectra were ac-

quired using both linear and reflectron mode. Each representative mass spectrum shown is average of 128–256 laser pulses. Mass calibration was performed internally using identified peptides FMRFamide (*m/z* 599.33) and SCP_A (*m/z* 1277.6) as calibrants. Laser power and delay time were optimized for each type of samples (i.e., single cells and LC fractions). Mass spectral peaks were assigned based on a combination of observed masses and the knowledge of prohormone sequences.

Northern analysis

Northern analysis was performed on *A. californica* as previously described (Fujisawa et al. 1999; Furukawa et al. 2001; Sweedler et al. 2002). RNA was isolated using the acid-phenol method (Chomczynski and Sacchi 1987). Northern blot analysis was performed on RNA using formaldehyde 3-(N-morpholino)propane-sulfonic acid (MOPS) denaturing agarose gels (1.5%) and downward transferred with 20× SSPE to positively charged nylon membranes (Biodyne B, Gibco BRL, Rockville MD). RNA was immobilized with UV (Stratalinker, Stratagene, La Jolla, CA) and visualized by staining with 0.02% methylene blue in 0.3 M sodium acetate (pH 5.5). Visualization of the RNA enabled confirmation that equal amounts of RNA were loaded in each lane and marking of the positions of RNA size standards (69956-3, Novagen, Madison WI) on the blot. After destaining with 1% SDS, 50 mM Na_3PO_4 (pH 7.2), and 1 mM EDTA, the blot was then prehybridized for 1 h at 50°C using 50% formamide, 10% dextran sulfate, 7% SDS, 250 mM Na_3PO_4 (pH 7.2), 10 mM EDTA, and 50 μg/ml salmon sperm DNA. Heat denatured random primed (New England Biolabs, Beverly, MA) ^{32}P dCTP labeled PRQFVa precursor cDNA probe was added, and hybridization continued overnight at the same temperature. Blots were washed two times for 15 min at room temperature with 2× SSPE 0.1% SDS and for 60 min at 50°C with 0.1× SSPE 0.1% SDS, and exposed to film. Autoradiographs and methylene blue stained blots were scanned into Photoshop and compiled to generate the final figure.

In situ hybridization

Whole mount ISH was performed on *A. californica* as previously described (Vilim et al. 2001). *Aplysia* CNS was isolated and digested with 1% protease type IX (Sigma-Aldrich, St. Louis, MO) for 1 h at 30°C to loosen connective tissue and facilitate removal of connective tissue. Following digestion, the ganglia were washed with ASW and fixed overnight at 4°C with 4% paraformaldehyde (Electron Microscopy Sciences, Fort Washington, PA) in PBS. The ganglia were washed with several changes of PBS/0.1% tween-20 (PBT) and desheathed. The ganglia were dehydrated in an ascending methanol series and stored in 100% methanol overnight at –20°C. Following rehydration in a descending methanol series, the ganglia were washed with PBS/0.3% triton and refixed for 20 min with 4% paraformaldehyde/PBS. The ganglia were washed with PBS, and the reactive groups were neutralized by washing first with 2 mg/ml glycine in PBS, then with 0.1 M triethanolamine HCl (pH 8.0; TEA-HCl), and finally with 1 ml TEA-HCl containing 2.5 μl acetic anhydride. Following several washes with PBT, the ganglia were prehybridized in Hyb-buffer (50% formamide, 5 mM EDTA, 5× SSC, 1× Dernhardts solution, 0.1% tween-20, 0.5 mg/ml yeast tRNA) overnight at room temperature and then 6–8 h at 50°C with fresh Hyb-buffer.

PRQFVa precursor mRNA was detected using the digoxigenin-labeled cRNA, alkaline phosphatase–labeled antibody to digoxigenin, and NBT/BCIP to develop the staining (Roche Molecular Biochemicals, Indianapolis, IN). Digoxigenin-labeled cRNA was synthesized with T7 RNA polymerase using the PRQFVa cDNA clone as a template and then used as probe (2 μg/ml of hyb-buffer). The ganglia were hybridized overnight at 50°C, then washed at 50°C (30 min each: 50% formamide/5× SSC/1% SDS; 50% formamide/2× SSC/1% SDS; 50% formamide/2× SSC/1% SDS; 0.2× SSC; 0.2× SSC) to remove unhybridized probe. The ganglia were washed three times for 10 min with PBT containing 0.2% BSA, and then blocked for 2 h with PBT containing 0.2% BSA and 10% normal goat serum (NGS). The ganglia were incubated overnight at 4°C with 1:200 dilution of alkaline phosphatase–conjugated anti-Dig antibody in PBT containing 0.2% BSA and 1% NGS. Following washes with PBT to remove unbound antibody, the ganglia were washed with detection buffer (100 mM NaCl, 50 mM $MgCl_2$, 0.1% Tween 20, 1 mM levamisol, 100 mM Tris-HCl, pH 9.5) and developed with 4.5 μl NBT and 3.5 μl BCIP in 1 ml of detection buffer. The staining reaction was visually monitored and stopped by washing with PBT when the level of staining was adequate. The stained ganglia were observed and photographed using a Nikon microscope (Morrell Instruments, Melville, NY) with epi-illumination against a white background. Photographs were taken with a Nikon CoolPix 990 digital camera attached to the microscope through a standard C-mount. Digital photographs were imported into Photoshop (Adobe Systems, San Jose CA), brightness and contrast were adjusted, and the photographs were compiled into figures.

Antibodies

Antibodies to PRQFVa were made in rats as described (Fujisawa et al. 1999; Furukawa et al. 2001). Briefly, the antigen was prepared by coupling PRQFVa (Anaspec) to BSA (Sigma A0281) using EDC (1-ethyl-3-(dimethylaminopropyl)carbodiimide, Sigma E7750). The coupling was performed in a 1 ml volume of 50 mM NaH_2PO_4 pH 7.2 containing 10 mg of BSA, 1 mg of peptide, and 25 mg of EDC. The mixture was allowed to react overnight at 4°C, and the coupled antigen was purified from the reaction using a Microcon-30 centrifugal ultrafiltration unit (spinning at 12,000*g* for 30 min at 4°C to concentrate). After washing the retentate four times with 0.4 ml of 50 mM NaH_2PO_4 (pH 7.2), it was resuspended in 0.5 ml of the same buffer and transferred to a new tube.

Two male Sprague-Dawley rats (Teconic, 250–300g) were immunized by intraperitoneal injection with either 6.5 μl (125 μg for rat 1) or 12.5 μl (250 μg for rat 2) antigen in an emulsion of 0.25 ml PBS and 0.25 ml of Freund's complete adjuvant. At 21 and 42 days after initial injection, the rats were boosted by intraperitoneal injection with either 3.25 μl (65 μg for rat 1) or 6.25 μl (125 μg for rat 2) antigen in an emulsion of 0.25 ml PBS and 0.25 ml of Freund's incomplete adjuvant. The animals were killed by decapitation at 49 days after initial injection, and the blood was harvested and processed for serum. Sera were aliquoted, frozen, and lyophilized, or stored at 4°C with EDTA (25 mM final) and thimerosal (0.1% final) added as stabilizers. The antibody generated by rat 1–labeled neurons do not contain PRQFVa, but do contain enterins (another FVamide neuropeptide that could cross react; Furukawa 2001). The antibody generated by rat 2 produced immunostaining that was more specific and was therefore used in all subsequent experiments.

Immunocytochemistry

Immunocytochemistry was performed on *A. californica* as previously described (Fujisawa et al. 1999; Furukawa et al. 2001; Vilim et al. 1996). Immunostaining was also performed on selected *A. kurodai* tissues to determine similarities of the two species. Tissues were fixed in freshly prepared fixative (4% paraformaldehyde, 0.2% picric acid, 25% sucrose, 0.1M NaH_2PO_4, pH 7.6) for either 3 h at room temperature or overnight at 4°C. Following washes with PBS to remove the fixative, the ganglia from large animals were desheathed to expose the neurons. Ganglia from small animals (10–15 g) were processed without desheathing. All subsequent incubations were done at room temperature with rocking. Tissue was permeabilized and blocked by overnight incubation in blocking buffer (BB: 10% normal donkey serum, 2% Triton X-100, 1% BSA, 154 mM NaCl, 10 mM Na_2HPO_4, 50 mM EDTA, 0.01% thimerosal, pH 7.4). Primary antibody was

diluted 1:250 in BB and incubated with the tissue for 4–7 days. The tissue was then washed twice a day for 2–3 days with washing buffer (WB: 2% Triton X-100, 1% BSA, 154 mM NaCl, 10 mM Na_2HPO_4, 50 mM EDTA, 0.01% thimerosal, pH 7.4). Following the washes, the tissue was incubated with 1:500 dilution of secondary antibody (Lissamine Rhodamine Donkey anti-Rat, Jackson ImmunoResearch Laboratories, West Grove, PA) for 2–3 days. The tissue was then washed twice with WB for 1 day and four times with storage buffer (1% BSA 154 mM NaCl, 10 mM Na_2HPO_4, 50 mM EDTA, 0.01% thimerosal, pH 7.4) for 1 day. The tissues were stored at 4°C or viewed and photographed on a Nikon microscope equipped with epifluorescence (Morrell Institute). Negatives were scanned and compiled into figures using Photoshop 3.0.

Measurements of muscle contractions

A. kurodai were anesthetized by injecting isotonic $MgCl_2$ solution. The anterior gut was dissected out of each animal, and longitudinal strip preparations (about 0.5 cm in width) were made. Spontaneous contractile activity of the strip preparation was recorded as described previously (Furukawa et al. 2001). The recording chamber (1.5 ml in volume) was filled with ASW having the following composition: 445 mM NaCl, 10 mM KCl, 10 mM $CaCl_2$, 55 mM $MgCl_2$, and 10 mM Tris-HCl (pH 8.0). To examine the action of fractions, a 15-μl aliquot prepared from a small amount of each fraction (1/100–1/500 of the total fraction volume) was injected into the chamber. Fractions containing ACN were dried and resuspended in ASW, while fractions from the cation exchange column were injected directly. To examine the dose-response relationship of synthetic peptide, an aliquot containing the known concentration of peptide was injected into the chamber, and final concentration of the synthetic peptide was calculated from the bath volume. To quantify these results, we first summed all the amplitudes of spontaneous contractions during 2 min before and after the application of peptide. Next, the ratio of the summed amplitudes was determined, converted to a percentage, and plotted against the concentration of peptide. In some experiments, the effect of the synthetic peptide on the anterior aorta of *A. kurodai* was also examined as described previously (Morishita et al. 2001). The contractile activity of a portion of the anterior aorta (about 1 cm in length) was measured as described above. A nerve innervating the anterior aorta (the vulvar nerve) was left intact, and the phasic contraction of the aorta was elicited by electrical stimulation of the vulvar nerve. The concentration-response relationship of the peptide for the phasic contraction of the aorta was analyzed by plotting the amplitude of the contraction against the concentration of peptide.

The concentration-response relationship was fitted to an equation of the form, $Y = A1 + (A2 - A1)/[1 + 10^{(\log X0 - X)p}]$. Y is the normalized response, X is a power for the concentration of the peptide (i.e., the concentration used is 10^X M), log$X0$ relates to EC_{50} (the concentration of peptide at which 50% response is expected), and p is a Hill coefficient. Curve fitting was done by the Levenberg-Marquardt algorithm using Origin (Microcal, Northampton, MA). Because the fitted values for p were usually between 1 and 1.3 in our data, we fixed it as 1 in the fittings shown in figures. Other constrains are described in figure legends.

CNS electrophysiology

The effects of PRQFVa on the excitability of neurons within the *A. californica* CNS were tested in a preparation that either consisted of the isolated cerebral and buccal ganglia with the cerebral-buccal connectives intact or with isolated buccal ganglia with the cerebral ganglia removed. In either case, ganglia were desheathed, exposing the cells of interest. Conventional intracellular recordings were made with glass microelectrodes filled with 2 M KAc and 30 mM KCl and beveled to 5–15 MΩ. Ganglia were pinned out in a Sylgard-lined dish with a volume of approximately 1.5 ml. The preparation was cooled to 14–17°C, constantly perfused at a rate of 0.33 ml/min with ASW alone (composition in mM: 460 NaCl, 10 KCl, 55 $MgCl_2$, 11 $CaCl_2$, and 20 HEPES buffer, pH 7.45–7.60), or ASW containing freshly dissolved PRQFVa.

RESULTS

Identification of PRQFVa

CNS extracts of *A. kurodai* contain several distinct fractions that have inhibitory actions on gut motility (Fujisawa et al. 1999; Furukawa et al. 2001). Figure 1*A* shows the initial HPLC profile of the CNS extract using a reversed-phase column. The bar indicates the fractions that contained the peptide described in this study. Following two further HPLC steps, the material was purified as a single absorbance peak (Fig. 1*B*). This purified substance inhibited spontaneous contractions of the *A. kurodai* gut (Fig. 1*C*). Amino acid sequencing showed that the substance is a peptide, with the following sequence (number in parenthesis indicates picomoles in each cycle): Pro (262.6), Arg (909.5), Gln (1967.2), Phe (1307.2), and Val (585.4). The mass number measured by FAB-MS was 645 ([M+H]+), suggesting C-terminal amidation. The structure of the purified peptide is therefore estimated to be PRQFVamide (PRQFVa). To confirm this structure, we carried out co-elution experiments of the purified peptide and the synthetic peptide. The retention time of PRQFVamide was identical to that of the native peptide in both reversed-phase and cationic exchange columns, and the mixture of the synthetic peptide and native

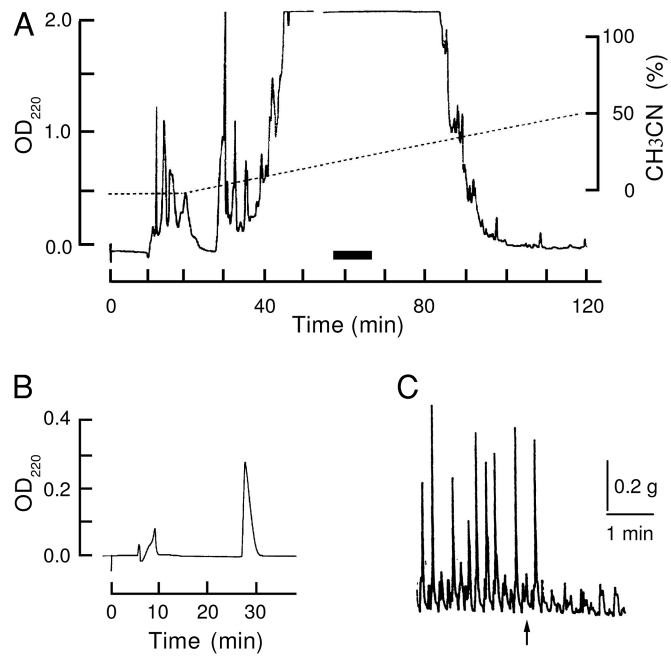

FIG. 1. Purification of Pro-Arg-Gln-Phe-Val-amide (PRQFVa) from CNS extracts of *Aplysia kurodai*. *A*: initial step of high-performance liquid chromatography (HPLC) fractionation by a reversed phase column. Retained material was eluted with a 200-min linear gradient of 0–100% of acetonitrile (CH_3CN) in 0.1% trifluoroacetic acid (TFA). As seen in this figure, most retained materials come out within 100 min. Fractions later shown to contain PRQFVa are indicated by a black bar. *B*: final purification step by a reversed phase HPLC. A retained substance was eluted isocratically with 13.8% CH_3CN/0.1% TFA. *C*: biological activity of the purified substance in the gut of *Aplysia*. A small aliquot containing 1/1,000 of the purified substance shown in *B* was injected into a recording chamber (arrow).

one eluted as a single absorbance peak in both columns (data not shown). We therefore conclude that the structure of the purified peptide is PRQFVamide.

Cloning of the PRQFVa precursor mRNA

Semi-nested degenerate RACE was performed from an *A. californica* ganglionic cDNA library using two vector primers and an antisense degenerate primer designed to PRQFVGKR. We assumed a glycine as the amide donor and a downstream Lys-Arg processing site to give the antisense degenerate primer more favorable annealing characteristics. The degenerate primer was used in semi-nested RACE from lambda cDNA library to define the sequence upstream of these peptides. Library screening identified an overlapping set of clones that were used to generate the consensus sequence. Sequencing of these cDNA clones resulted in a 3790-bp consensus sequence (GenBank accession AY231295). Northern analysis (see Fig. 6) revealed that the mRNA is approximately 4 kb comparison with the positions of RNA size markers, thus suggesting that the consensus sequence is near full length.

The predicted mRNA contained a 2586-bp open reading frame that codes for an 862 amino acid precursor shown in Fig. 2. The precursor had a predicted signal peptide and a predicted cleavage site between Ala(26) and Gln(27) (Nielsen et al. 1997), indicating that the protein is targeted to the secretory pathway. Analysis of the precursor structure predicts that it codes for a total of 33 copies of PRQFVa and four related pentapeptides. All of them are expected to be amidated peptides as indicated by C-terminal glycines (Eipper et al. 1992) and furin-like consensus cleavage sites (Seidah and Chretien 1999).

MALDI-MS detection of PRQFVa precursor-derived peptides in abdominal neurons

MALDI analysis was performed on the abdominal ganglion cells of *A. californica*, which were shown to be PRQFVa positive by both immunostaining and ISH (see *Distribution of PRQFVa in the CNS and peripheral tissues*). Isolated neurons were transferred to a MALDI sample plate for peptide analysis. Sample preparation and mass spectrometric measurements were performed as previously described (Fujisawa et al. 1999). Figure 3 shows a representative MALDI mass spectrum in the 550–900 Da range from isolated abdominal ganglion neurons. PRQFVa and four related peptides predicted from the precursor were detected as well as FMRFamide (Scheller) and *Aplysia* MIP related products (AMRPs) (Fujisawa et al. 1999). Note that one of the AMRPs, GAPRFVamide, has the same mass as PRQFVa, therefore complicating the assignment of this peak (see DISCUSSION).

Distribution of PRQFVa in the CNS and peripheral tissues

The gross distribution of the PRQFVa mRNA in the CNS of *A. californica* was determined using Northern analysis. This analysis was conducted on total RNA obtained from specific ganglia of five animals. Northern analysis (Fig. 4) shows that PRQFVa precursor mRNA is unevenly distributed throughout the central ganglia of *Aplysia* and is approximately 4 kb in length. The relative abundance of PRQFVa mRNA in the CNS is abdominal $\gg$ pedal $>$ pleural $>$ buccal ganglia. More

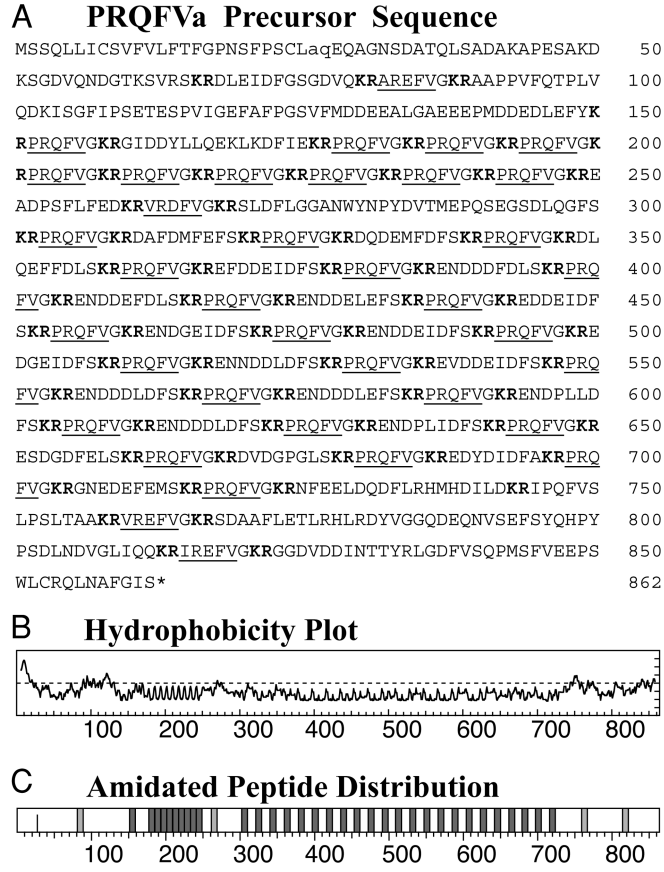

FIG. 2. Predicted amino acid sequence and structure of the PRQFVa precursor protein. *A*: amino acid sequence of the PRQFVa precursor protein in *A. californica*. Amino acids are numbered at right, and predicted amidated peptides are underlined. Mono- and dibasic cleavage sites are shown in bold, and lowercase letters denote predicted signal sequence cleavage site (CLa-qEQ). The precursor contains 33 copies of PRQFVa and 4 other structurally related amidated pentapeptides. *B*: hydrophobicity plot of the PRQFVa precursor with amino acids numbered at the bottom. Hydrophobicity increases above the dotted line and hydrophylicity increases below the dotted line. Notice the initial hydrophobic stretch that indicates the signal sequence and the highly repetative nature of the precursor. *C*: scale drawing the distribution of the predicted peptides on the precursor with amino acids numbered at the bottom. Copies of PRQFVa (33 in all) are shown as dark gray bars, and the lighter gray bars are AREFVamide, VRDFVamide, VREFVamide, and IREFVamide (respectively, from *left* to *right*). Connecting peptides are shown unshaded, and the half height line denotes the position of the predicted signal cleavage site.

detailed information about the distribution of PRQFVa containing neurons and their processes was obtained using a combination of ISH and IMM. Correlation between immunostaining and ISH staining was used to assess the specificity of these two methods (Eberwine et al. 1994). PRQFVa immunopositive neurons showed a corresponding distribution PRQFVa ISH positive neurons (illustrated as gray circles in diagrams of Figs. 5–7), indicating that the antibody to PRQFVa is specific. Additionally, immunostaining with this antibody was abolished by preincubation with 10^{-4} M PRQFVa (data not shown). However, there were clearly PRQFVa ISH positive neurons that were not PRQFVa immunopositive (illustrated as open circles in diagrams of Figs. 5–7), complicating the interpretation of PRQFVa ISH signals (see DISCUSSION).

There was some variability in the number and size of neurons staining in different animals, even in the same weight range. What we present are the typical results from both large

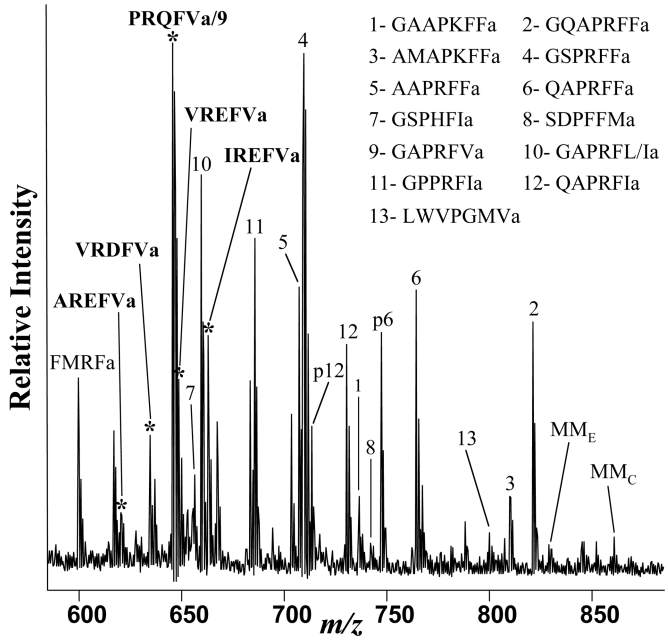

FIG. 3. MALDI TOF mass spectrum (550–900 Da range) from isolated *A. ccalifornica* abdominal ganglion neurons. Detection of the mass peaks predicted by the putative amidated peptides on the PRQFVa precursor confirms that they are processed from the precursor. Assigned peaks are labeled with corresponding peptides. Peptides derived from 2 other precursors, FMRFamide and *Aplysia* MIP related peptide AMRPs, are also detected. Peaks corresponding to the products of the PRQFVa precursor are shown with an asterisk. Peaks labeled with a number correspond to amidated AMRPs as indicated in the *inset*. P indicates a pGlu-modified form of the 2 AMRPs containing N-terminal Gln.

and small animals. A diagram summarizing the distribution of PRQFVa positive neurons in each ganglion represents the correlated results of ISH staining and immunostaining (shown as gray circles). Positions of neurons that exhibited PRQFVa ISH staining without corresponding IMM staining are shown with unfilled circles. Locations of the nerves in the drawings are intended as landmarks, the relative positions of the neurons and nerves vary somewhat from animal to animal and depend on how the ganglia are pinned. To avoid redundancy, neurons that were observed to be both immunopositive and ISH positive are referred to as PRQFVa positive. Since ISH cannot be used to define processes of neurons, cross-correlation is not possible. However, it is likely that immunostaining of processes reflects the presence of bona fide PRQFVa because all the immunostained neuronal cell bodies are correlated with ISH stained neuronal cell-bodies. The Northern analysis, ISH, and IMM shown were performed on *A. californica*. *A. kurodai* showed similar distribution of immunostaining in the CNS, gut, and vasculature (data not shown).

Buccal ganglion

In the buccal ganglion, there are three neurons on the caudal surface that are PRQFVa positive by both immunostaining and ISH (Fig. 5*B*). Two of these neurons are bilaterally symmetrical and one is asymmetrical. The asymmetrical neuron is typically observed lateral in the right side of the buccal ganglion, which is the left hemiganglion in the animal. In addition, a cluster of small neurons on the rostral surface is weakly ISH positive (Fig. 5*A*). Immunostaining does not show any apparent PRQFVa immunopositive neurons that correspond to these PRQFVa ISH positive neurons. PRQFVa immunopositive processes are observed throughout the neuropile of the buccal ganglion, and some PRQFVa immunopositive axons are observed in all the buccal nerves.

Cerebral ganglion

The dorsal and ventral surfaces of the cerebral ganglion contain several symmetrical PRQFVa positive neurons. On the dorsal surface, a symmetrical pair of IMM and ISH positive neurons is observed near the base of the optic and posterior tentacular nerves (Fig. 5*C*). A symmetrical pair of IMM and ISH positive neurons is also observed in the deeper layers of the G cluster (nomenclature of clusters according to Jahan-Parwar and Fredman 1976 and Phares and Lloyd 1996). Scattered smaller ISH and IMM positive neurons are observed in the F and C clusters. There are also some neurons in the F and C clusters that are ISH positive but have no apparent IMM positive counterparts. In the posterior part of the cerebral ganglion, a cluster of small intensely stained IMM and ISH positive cells are present in the D cluster. Neurons in the A cluster are weakly IMM and ISH positive. On the ventral surface, IMM and ISH positive neurons can be observed in the center of the ganglion, E cluster (Fig. 5*D*). A band of IMM and ISH positive neurons are observed in the deeper layers of the B cluster. A cluster of ISH positive neurons that has no apparent IMM positive counterpart can be observed in the D cluster. Several additional scattered ISH positive neurons that have no apparent IMM positive counterpart can also be observed throughout the ganglion. PRQFVa immunopositive processes are observed throughout the neuropile of the cerebral ganglion, including the neuropile of the M and E cluster, and some PRQFVa immunopositive axons are observed in all the nerves of the cerebral ganglion.

Pleural and pedal ganglion

There are two neurons in each pleural ganglion that are PRQFVa positive with both IMM and ISH (Fig. 6). In the left pleural ganglion, there are also a number of ISH positive neurons that do not have a corresponding distribution of IMM positive neurons. PRQFVa immunopositive processes can be observed in the neuropile of the pleural ganglion, and immu-

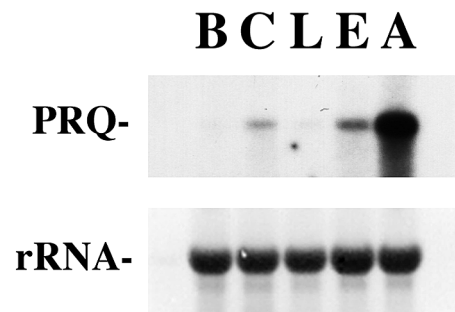

FIG. 4. Northern blot of ganglionic distribution of PRQFVa mRNA. rRNA: methylene blue staining of RNA transferred on the Northern blot shows equal loading of total RNA in all lanes. *Aplysia* ribosomal RNA runs as a single18s band. PRQ: Northern blot hybridization of total RNA isolated from each of the 5 ganglia with a cDNA probe of the PRQFVa precursor. Hybridizing band runs at approximately 4 kb. B, buccal ganglion; C, cerebral ganglion; L, pleural ganglion; E, pedal ganglion; A, abdominal ganglion.

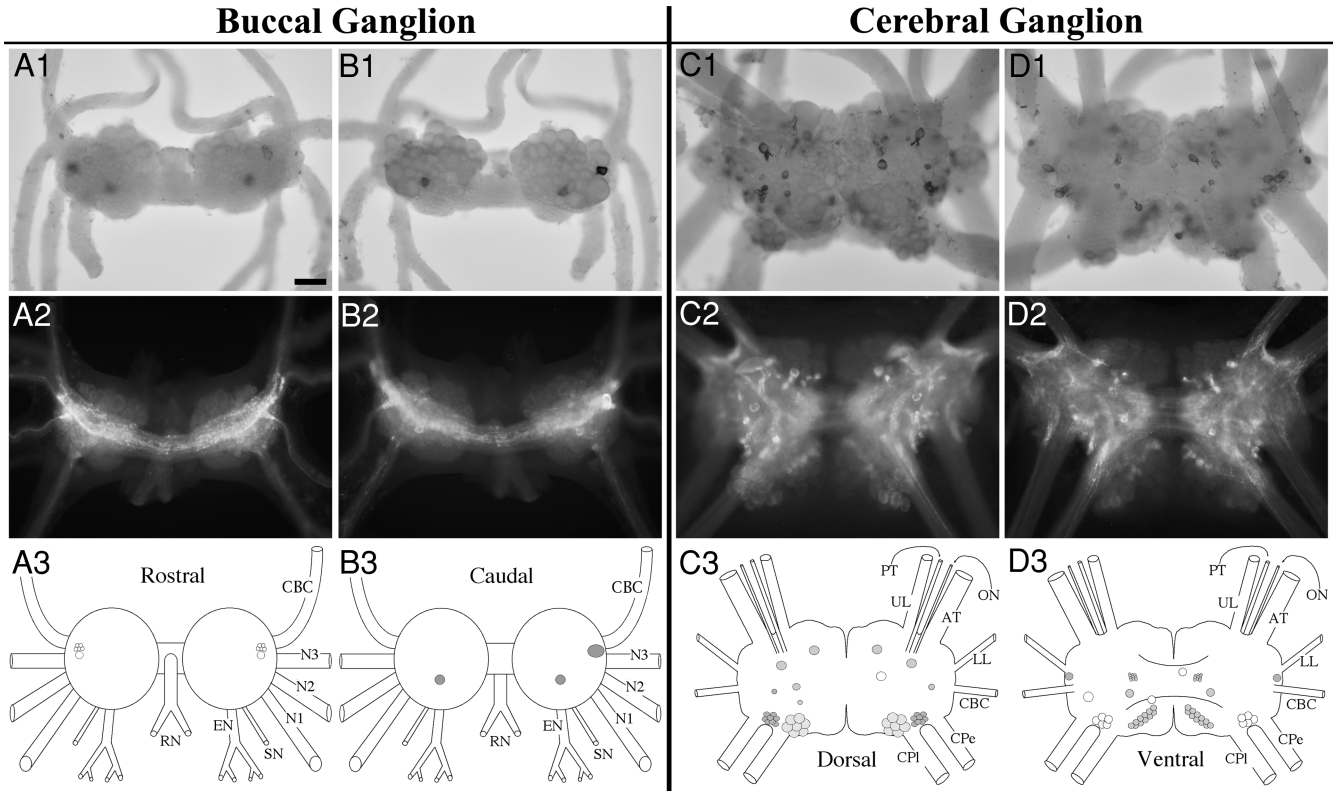

FIG. 5. PRQFVa in the buccal and cerebral ganglion. *A1*: in situ hybridization of rostral surface. *A2*: immunocytochemistry of rostral surface. *A3*: drawing of the rostral surface of the buccal ganglion. *B1*: in situ hybridization of the caudal surface. *B2*: immunocytochemistry of caudal surface. *B3*: drawing of the PRQFVa-positive neurons on the caudal surface of the buccal ganglion. CBC, cerebrobuccal connective; N1, nerve 1 (B4); N2, nerve 2 (B5); N3, nerve 3 (B6); SN, salivary nerve (B3); EN, esophageal nerve (B2); RN, radula nerve (B1). *C1*: in situ hybridization of the dorsal surface. *C2*: immunocytochemistry of the dorsal surface. *C3*: drawing of the PRQFVa neurons on the dorsal cerebral ganglion. *D1*: in situ hybridization of the ventral surface. *D2*: immunocytochemistry of the ventral surface. *D3*: drawing of the PRQFVa neurons on the ventral surface of the cerebral ganglion. UL, upper labial nerve; PT, posterior tentacular nerve; ON, optic nerve; AT, anterior tentacular nerve; LL, lower labial nerve; CBC, cerebrobuccal connective; CPe, cerebropedal connective; CPl, cerebropleural connective. Neurons drawn in darker shades of gray stain more intensely. (Scale bar in *A1* is 200 μm and is the same for all panels).

nopositive axons can be observed in all of the pleural nerves. In the pedal ganglion, there are numerous neurons that are PRQFVa positive with both IMM and ISH. On the dorsal surface, a cluster of PRQFVa positive neurons is observed near the pleural-pedal connective. On the ventral surface of the pedal ganglion, there is a cluster of PRQFVa positive neurons near the pleural-pedal connective extending toward pedal nerves 5 and 6. There are also two other clusters of PRQFVa positive neurons, one at the base of pedal nerve 9 and the other near to the center of the ganglion. There are also several clusters of PRQFVa ISH-staining neurons that do not have a corresponding distribution of PRQFVa immunostaining neurons: one on the ventral surface near the cerebral-pedal connective and one on the ventral surface near the center of the ganglion. PRQFVa immunopositive processes can be observed in the neuropile of the pedal ganglion and immunopositive axons can be observed in all of the pedal nerves.

Abdominal ganglion

Consistent with the ganglionic distribution of PRQFVa mRNA observed by Northern blot, the density of PRQFVa positive neurons was greatest in the abdominal ganglion (Fig. 7). On the dorsal surface, there is a cluster of large PRQFVa positive neurons located in the left upper quadrant. Another cluster of PRQFVa positive neurons is observed in the lower left quadrant on the dorsal surface. On the ventral surface, a cluster of PRQFVa positive neurons is observed in the left side, which is the right hemiganglion in the animal. Also on the ventral surface, two apparently bilaterally symmetrical clusters of small neurons are observed laterally near the middle of the ganglion. PRQFVa ISH positive neurons that are not to the PRQFVa immunopositive can be observed on the dorsal surface in the upper left quadrant and in the lower right quadrant. Additional PRQFVa ISH positive neurons without corresponding PRQFVa immunoreactivities are observed on the ventral surface near the middle of the right side on the ventral surface, which is the left hemiganglion in the animal. PRQFVa immunopositive processes can be observed in the neuropile of the abdominal ganglion and immunopositive axons can be observed in all of the nerves of the abdominal ganglion, with particularly intense staining in the branchial nerve.

Peripheral tissues

Since PRQFVa was identified based on its ability to modulate contractions of the gut, we sought to determine whether the gut did in fact contain this peptide and where in the gut it might be located. The majority of PRQFVa immunostained processes appeared to be associated with the gut vasculature (Fig. 8,

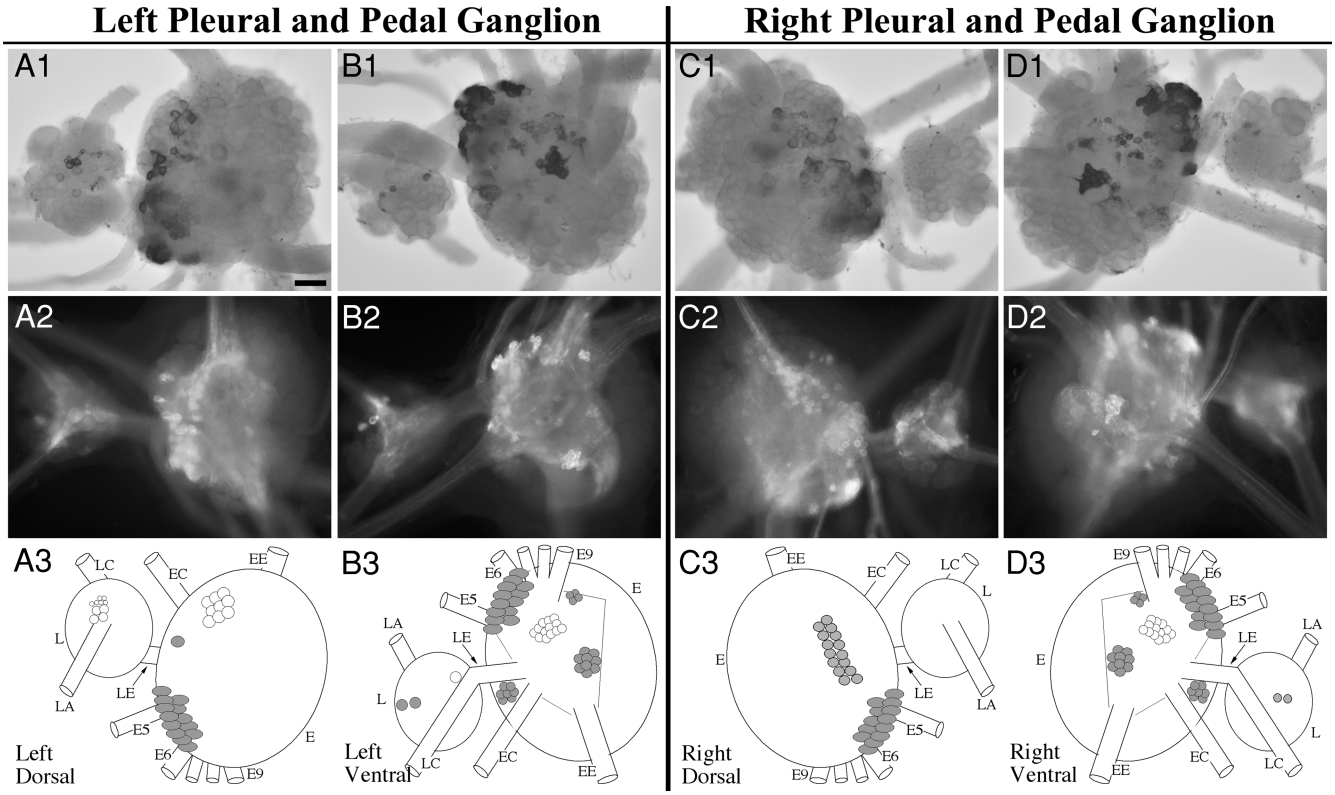

FIG. 6. PRQFVa in the pleural and pedal ganglion. *A1*: in situ hybridization of the left ganglion pair dorsal surface. *A2*: immunocytochemistry of the left ganglion pair dorsal surface. *A3*: drawing of the PRQFVa neurons on the dorsal surface of the left ganglion pair. *B1*: in situ hybridization of left ganglion pair ventral surface. *B2*: immunocytochemistry of the left ganglion pair ventral surface. *B3*: drawing of the PRQFVa neurons on the ventral surface of the left ganglion pair. *C1*: in situ hybridization of right ganglion pair dorsal surface. *C2*: immunocytochemistry of the right ganglion pair dorsal surface. *C3*: drawing of the PRQFVa neurons on the dorsal surface of the right ganglion pair. *D1*: in situ hybridization of right ganglion pair ventral surface. *D2*: immunocytochemistry of the right ganglion pair ventral surface. *D3*: drawing of the PRQFVa neurons on the ventral surface of the right ganglion pair. L, pleural ganglion; E, pedal ganglion; LE, pleuropedal connective; EE, pedal commisure; EC, cerebropedal connective; LC, cerebropleural connective; LA, pleuroabdominal connective; E5, posterior tegumentary nerve (P5); E6, anterior parapodial nerve (P6); E9, posterior pedal nerve (P9). Not all nerves are drawn for simplicity. (Scale bar in *A1* is 200 μm and is the same in all panels.)

E–H), although some immunostained processes were observed in association with the musculature of the crop (Fig. 8*F*). We did not observe any PRQFVa immunostained cell bodies in the gut, but immunostained axons were observed in nerves within the gut and in the stomatogastric ring (Fig. 8*G*) (Fujisawa et al. 1999). Dense PRQFVa immunostained processes were also observed in the gastroesophageal artery (Fig. 8*A*), the main artery of the gut. The vasculature of the gill (Fig. 8*C*) and kidney (Fig. 8*D*) also contained PRQFVa immunostained processes. PRQFVa immunostained axons were observed in nerves of the body wall (Fig. 8*B*), and some immunostained processes were also observed, but it was difficult to determine if they were associated with the musculature or the vasculature of the body wall. A similar distribution of immunostained processes was observed in the gut and vasculature of *A. kurodai* (data not shown).

Physiological actions of PRQFVa

GUT. Because PRQFVa was purified by bioassay using the gut of *A. kurodai*, we first examined the dose-response relationship of the action of synthetic PRQFVa in this tissue. The longitudinal strip preparation of the gut of *A. kurodai* shows spontaneous contractile activity. Overall activity of this preparation is rather stable despite the variability in the amplitude of each contraction. We quantified the contraction of the gut as described in METHODS and constructed a does-response curve (Fig. 9). PRQFVa inhibited spontaneous contractions of the gut in a dose-dependent manner. Activity almost ceased when 10^{-6} M PRQFVa was applied (Fig. 9*A*). Threshold concentration for the inhibitory action of PRQFVa was close to 10^{-9} M, and the EC_{50} was 1.6×10^{-7} M (Fig. 9).

ANTERIOR AORTA. As described above, many of the PRQFVa-immunopositve fibers in the peripheral tissues seem to be associated with the vasculature. We therefore examined the effect of PRQFVa on the contractile properties of one of the major arteries in the *Aplysia* cardiovascular system, the anterior aorta. Because the isolated anterior aorta is usually quiescent, the contraction of the musculature in the aorta was evoked by electrical stimulation of the vulvar nerve that innervates the aorta (Sawada et al. 1981). Figure 10 illustrates the effect of PRQFVa on phasic contractions of the anterior aorta in *A. kurodai* caused by electrical stimulation of the vulvar nerve. In response to pulse stimulation (5 V, 1 ms, 10 Hz) for 1 s, a phasic contraction of the aorta was evoked (Fig. 10*A*). The phasic contraction of the aorta was inhibited in the presence of PRQFVa. A threshold concentration for the action was

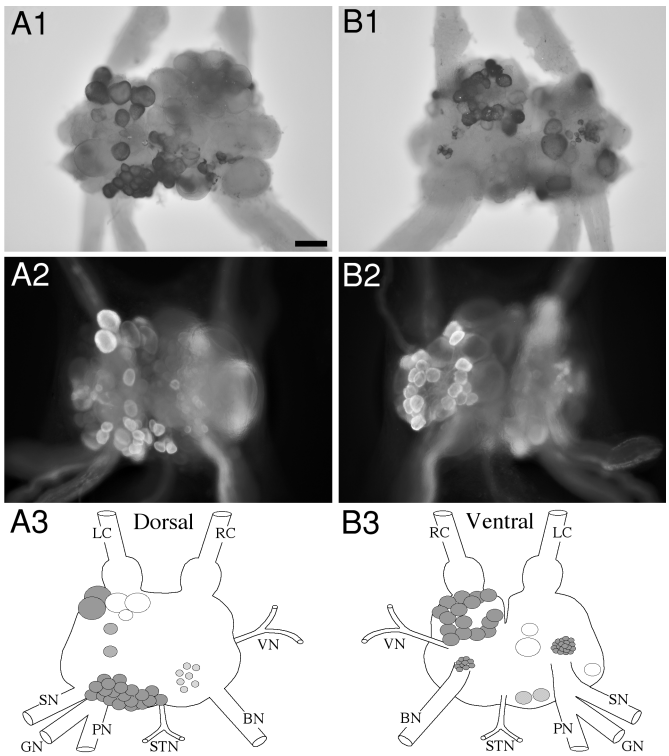

FIG. 7. PRQFVa in the abdominal ganglion. *A1*: in situ hybridization of the dorsal surface. *A2*: immunocytochemistry of dorsal surface. *A3*: drawing of the PRQFVa neurons on the dorsal surface of the abdominal ganglion. *B1*: in situ hybridization of the ventral surface. *B2*: immunocytochemistry of the ventral surface. *B3*: drawing of the PRQFVa neurons on the ventral surface of the abdominal ganglion. LC, left pleuroabdominal connective; RC, right pleuroabdominal connective; VN, vulvar nerve; BN, branchial nerve; STN, spermathecal nerve; PN, pericardial nerve; GN, genital nerve; SN, siphon nerve. Neurons that are drawn in darker shades of gray stain more intensely. (Scale bar in *A1* is 200 μm.

$<10^{-7}$ M. In contrast to the effect of PRQFVa on the gut, the inhibition caused by PRQFVa on the aorta was incomplete even at 10^{-5} M. According to the fitting shown in Fig. 10*B*, 26% of the contraction was assumed to be not affected by PRQFVa (Fig. 10). The estimated EC_{50} was 4×10^{-7} M. The application of an *Aplysia* cardioactive peptide, NdWFamide, evokes a sustained contraction of the anterior aorta (Morishita et al. 2001). When PRQFVa was co-applied with NdWFamide, the sustained contraction was partly relaxed (data not shown).

BUCCAL NEURONS. We sought to determine whether PRQFVa had any effect on the excitability of neurons within the feeding central pattern generator (CPG). We examined three neurons, each of which is associated with a specific movement in feeding behavior: the protraction motor neurons B31/32, the radular closure neuron B8, and the multifunctional retraction neurons B4/5 (Jahan-Parwar et al. 1983; Morton and Chiel 1993; Susswein and Byrne 1988). In each case, neurons were impaled with two electrodes, one of which was used for voltage recording and one for current injections. For B31/32 and B8, 10 nA (B31/32) and 2 nA (B8) of depolarizing current was injected for 4 s, whereas for B4/5, 3 nA of depolarizing current was injected for only 2 s. In all cases, depolarizing pulses were applied every 30 s. PRQFVa was perfused into the bath at increasing concentrations (from 10^{-7} to 10^{-5} M). PRQFVa reversibly reduced the firing rate of B31/32 ($n = 4$) and B4/5 ($n = 3$) in a concentration-dependent manner, but did not affect B8 firing frequency ($n = 3$). An overall statistically significant difference was observed between varying concentrations of PRQFVa in the bath for B31/32 and B4/5 [single factor ANOVA; B31/32: $F(4, 15) = 8.035$, $P < 0.001$; B4/5: $F(4, 10) = 63.873$, $P < 0.001$], but not B8. When individual comparisons were made between peptide present and control or wash, we found a statistically significant decrease of B31/32 and B4/5 excitability whenever PRQFVa was in the bath (*t*-test, unequal variances, $P < 0.01$).

DISCUSSION

In this paper we described the purification of a novel pentapeptide PRQFVa and the cloning of the cDNA that encodes the precursor to this peptide and four additional structurally related pentapeptides. We also mapped the distribution of these peptides in both the CNS and peripheral tissues of *Aplysia* using in situ hybridization and immunocytochemistry. Finally, we characterized the bioactivity of PRQFVa in the gut, vasculature, and selected buccal neurons.

Biochemistry

Five structurally related pentapeptides are predicted by the processing sites that are present on the precursor. One pentapeptide (PRQFVa) is present in 33 copies on the precursor, and the other four pentapeptides (AREFVamide, VRDFVamide, VREFVamide, and IREFVamide) are present as single copies. All five predicted peptides are amidated and share three invariant amino acids. Specifically, the second amino acid is an arginine, the fourth is a phenylalanine, and the fifth is a valine. A loose homology is also present in the third position in which glutamine is present in the most abundant peptide, PRQFVa, and is replaced by glutamate or aspartate in the other four peptides that are present as single copies on the precursor.

To determine whether the predicted peptides, (especially the 4 that were not purified and sequenced) are processed from the precursor, we profiled the peptides in abdominal neurons using MALDI-TOF-MS. This technique allows detection of very small amounts of neuropeptides based on accurate measurements of their molecular masses. MALDI-TOF-MS is particularly powerful when it is combined with sequence information derived from biochemical and molecular studies. Specifically, when the weights of several of the predicted precursor products are all present in a given cell(s), the confidence of the peptide assignment as a precursor product is greatly enhanced. Thus the likelihood that a single product is an artifact or represents a product with a different structure, but the same molecular weight is relatively low. Finally, because of its accuracy, MALDI-TOF-MS can be used to determine the presence of posttranslational modifications of neuropeptides.

MALDI-TOF-MS analysis was performed on clusters of abdominal neurons in which ISH and immunocytochemistry indicated the possible presence of PRQFVa and related peptides. We detected peaks with masses that correspond to the five peptides. However, in addition to these peptides, we also detected molecular masses that corresponded to another peptide family, the AMRPs. None of the four PRQFVa-related peptides that are present in single copies have a molecular weight that corresponds to the molecular weights of any of the AMRPs, and therefore these four peptides do not represent any of the AMRPs. However, the molecular mass of PRQFVa is

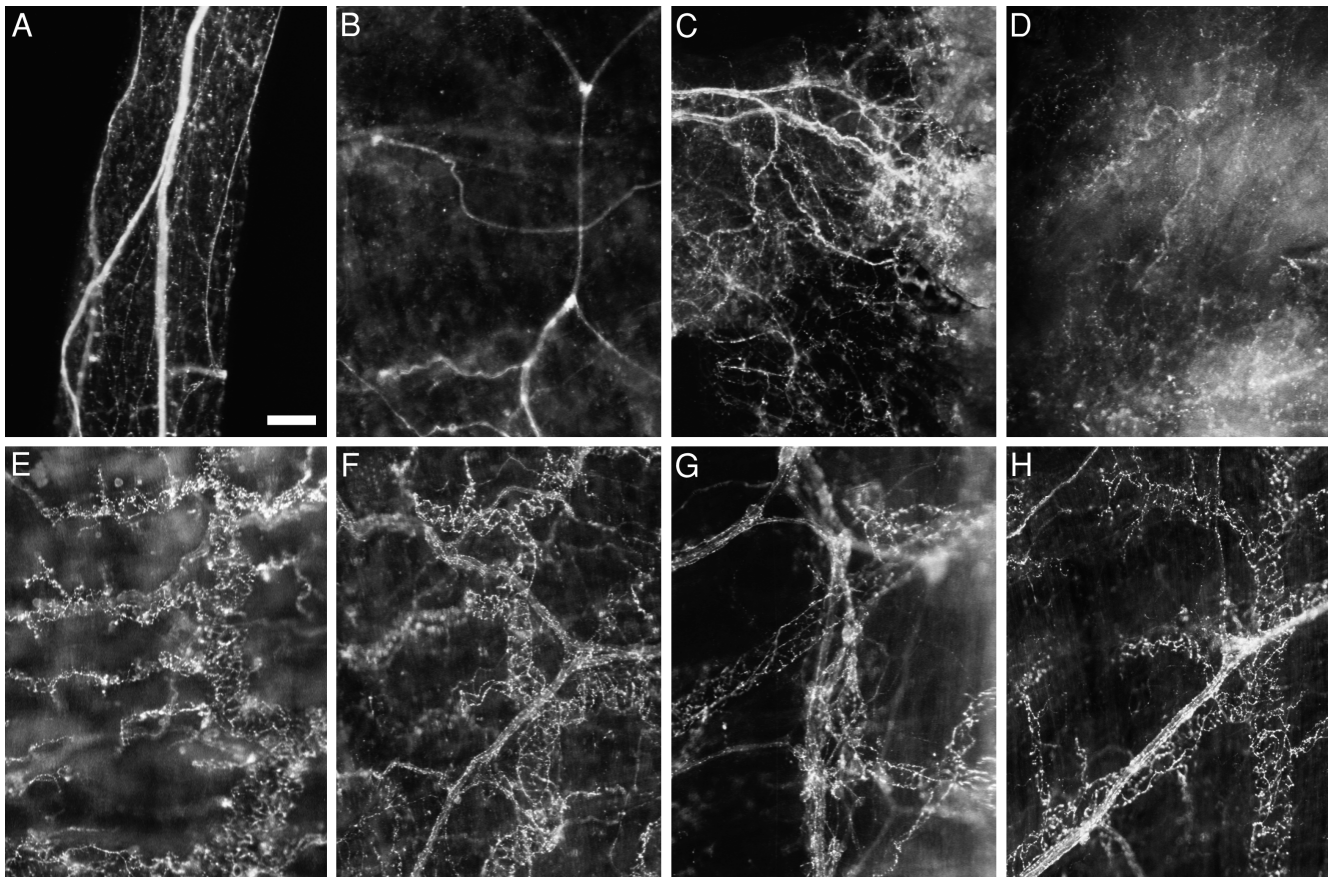

FIG. 8. PRQFVa immunostaining in peripheral tissues. *A*: gastroesophageal artery. *B*: body wall. *C*: gill. *D*: kidney. *E*: esophagus. *F*: crop. *G*: stomatogastric ring (vertical center). Crop is at *left* and triturating stomach is at *right*. *H*: filtering chamber. Immunoreactive fibers appear to be predominantly associated with vasculature in peripheral tissues, although some immunoreactive fibers may be associated with muscle (e.g., in the crop and body wall). Scale bar in *A* is 200 um.

identical to that of one of the members of the AMRP family, the hexapeptide GAPRFVa. There are several observations that indicate that the PRQFVa peak does reflect bona fide PRQFVa. First, the peptide was purified and sequenced from CNS extracts, providing evidence for the synthesis of PRQFVa in the CNS. Second, the intensity of the PRQFVa peak appears to be too large to be completely accounted for by GAPRFVamide. Even though MALDI is only semi-quantitative, signal intensity often correlates with the molar ratios of peptides derived from

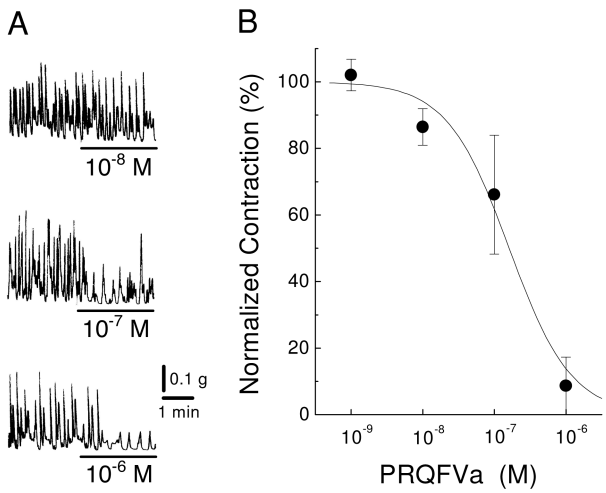

FIG. 9. PRQFVa inhibits contractions of the gut. *A*: effect of PRQFVa on the spontaneous contraction of the gut. *B*: concentration-response relationship of the inhibitory action of PRQFVa. A normalized contraction was obtained as described in METHODS and plotted against the peptide concentration. Each symbol shows a mean of 4 preparations, and a vertical bar indicates SE of the mean. A smooth line is a best fit of the equation described in METHODS. For this curve fitting, A1, A2, and p were fixed to 0, 100, and −1, respectively. Estimated logX0 was −6.8.

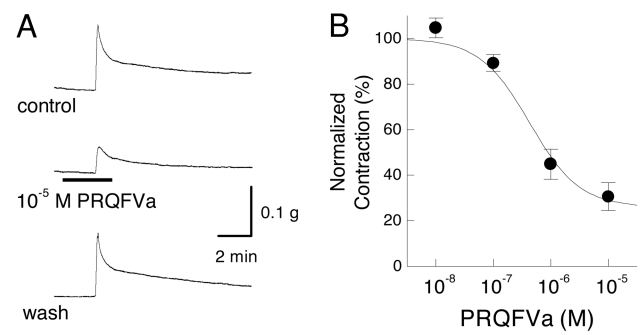

FIG. 10. PRQFVa attenuates contractions of the anterior aorta. *A*: effect of PRQFVa on phasic contractions of the anterior aorta elicited by repetitive stimuli (5 V, 1 ms, 10 Hz, 1 s) of the vulvar nerve. *B*: dose-response relationship of the inhibitory action of PRQFVa. The peak amplitude of the evoked contraction in the presence of PRQFVa was normalized to the one in the absence of the peptide and plotted against the peptide concentration. Each symbol shows a mean of 4 preparations, and a vertical bar indicates SE. A smooth line is a best fit of the equation described in METHODS. For this curve fitting, A2 and p were fixed to 100 and −1, respectively. Estimated A1 and logX0 were 26.0 and −6.4, respectively.

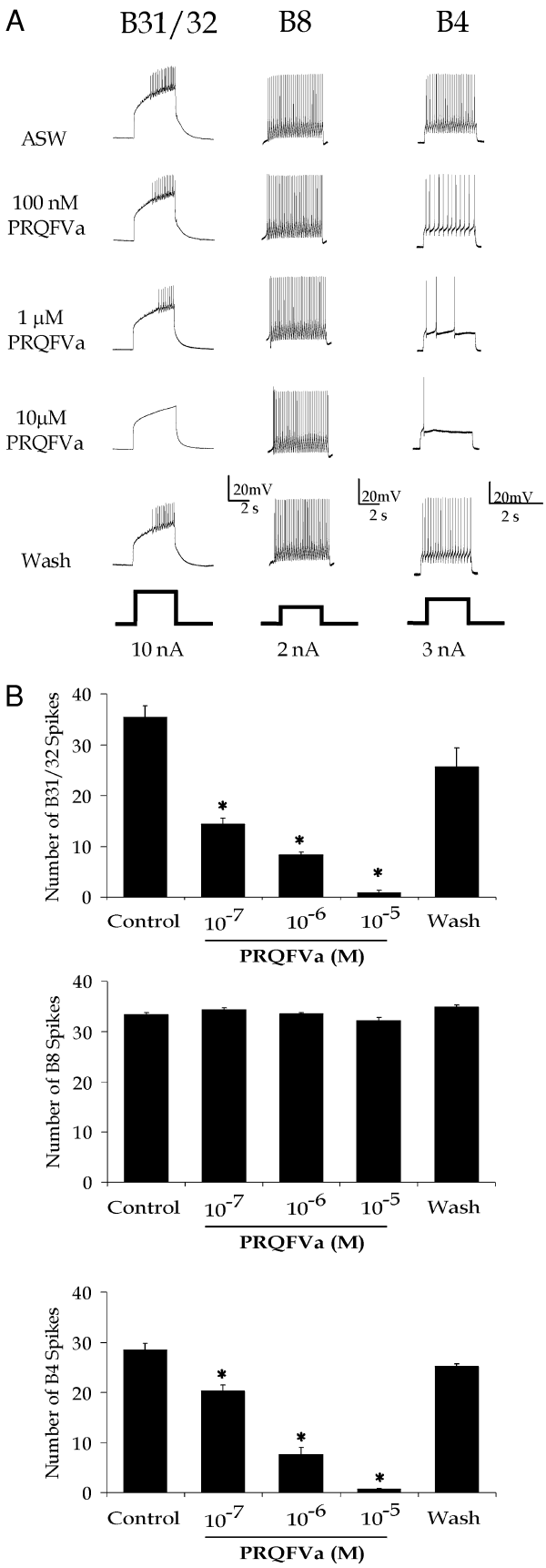

a single precursor. Note that the PRQFVa/GAPRFVamide peak is of greater intensity than that GSPRFFamide that is present in 11 copies on the AMRP precursor compared with only 2 copies of GAPRFVamide. The generation of PRQFVa could account for the greater intensity of the PRQFVa/GAPRFVamide peak. Third, the processing sites for all the predicted peptides on the precursor are the same, KR. Thus for PRQFVa not to be generated one would have to postulate that while the KR sites used for processing the PRQFVa-related peptides, the KR sites on the same precursor associated with PRQFVa peptide are not.

Localization and bioactivity

We used two methods to determine the localization of PRQFVa neurons. The two methods ISH and IMM are complementary; each has its advantages and shortcomings. Although ISH detects the presence of mRNA, in most cases it can only be used to detect neuronal somata. As in the case of neuropeptide-expressing neurons, the mRNA encoding the neuropeptide precursor is abundantly expressed, resulting in a high signal to noise ratio for ISH and giving ISH a high degree of specificity. The strength of IMM is that, unlike ISH, it can be used to detect the antigen not only in the somata but also in processes. In the case of peptides, the weakness of IMM is that it is susceptible to false positives from peptides with similar epitopes that are encoded by different genes. Since IMM and ISH were performed on different preparations, we can only compare the distribution of neurons with the two techniques. Similarities in distribution can provide evidence for the specificity of the antibody, but cannot definitively show that all the same neurons are staining with IMM and ISH.

The observation that the distribution of PRQFVa immunostained neurons had a corresponding distribution of PRQFVa ISH-stained neurons provides evidence that the antibody generated to PRQFVa is specific. However, there are a few instances where some of the PRQFVa ISH-stained neurons did not have a corresponding distribution of PRQFVa immunostained neurons. There are several possible explanations for this mismatch. Since the ISH was performed using an antisense cRNA of the entire mRNA sequence, cross-hybridization to an unrelated mRNA is possible. Another plausible explanation is that the PRQFVa gene is alternatively spliced to encode a neuropeptide precursor that produces neuropeptides that are structurally dissimilar to PRQFVa and do not bind the antibody to PRQFVa. On the other hand, these neurons may in fact contain the mRNA that encodes the PRQFVa precursor, but may not contain enough of the peptide in the cell body to produce staining that is above background levels. Possible reasons for this include a low level of synthesis, a high rate of transport out of the cell body, or an absence of the enzymes

FIG. 11. PRQFVa decreases the excitability of specific neurons within the buccal CPG. *A*: sample recordings of the protraction motor neuron B31/32, the radular closure motor neuron B8, and the multifunctional retraction neuron B4/5 (each neuron is recorded in different preparations). For B31/32 and B8, 10 nA (B31/32) and 2 nA (B8) of current were applied for 4 s every 30 s. In the case of B4/5, a 2-s depolarizing pulse of 3 nA was applied every 30 s. Bath application of PRQFVa reduced the firing rate of B31/32 and B4/5 in a concentration-dependent manner. *B*: group data (mean ± SE; $n = 3$), showing the inhibitory effects of PRQFVa on B31/32 and B4/5, but not on B8 excitability. An asterisk indicates a statistically significant reduction from control values.

required for the posttranslational modifications that produce the mature peptide. At present, we cannot determine the exact reasons for the additional PRQFVa ISH-staining neurons.

On a more global level, the PRQFVa distribution observed using immunostaining was consistent with the distribution observed with Northern analysis. For instance, in Northern analysis, the level of PRQFVa mRNA in the buccal and pleural ganglia was below the level of detection (Fig. 4), and only one or two neurons were detected (Figs. 5 and 7) in these ganglia using immunostaining and ISH staining. On the other hand, the abdominal ganglion contained clusters of PRQFVa-staining neurons and this ganglion produced a strong signal in Northern analysis. The consistency of the distribution of PRQFVa-immunostained neurons with the distribution observed in the northern blot provides additional evidence that the antibody to PRQFVa is specific. Thus we can be reasonably confident that the staining observed with the PRQFVa antibody reflects the actual distribution of this peptide. It is important to validate the immunostaining of the peptide because ISH can only be used to map the distribution of peptide precursor expressing neuronal soma, not their axons and processes. Immunostaining is also generally easier to perform and can be more easily used to determine if dye-marked electrophysiologically identified neurons express the peptide.

Consistent with the possible role of PRQFVa in the control of feeding behavior, immunostaining was observed both in the somata and in the neuropile of the buccal ganglion. Furthermore, staining was observed in the neurons and neuropile of the cerebral ganglion. This included staining of the neuropile in the M cluster, a cluster that contains both command-like neurons and neurons that modulate the activity of the feeding CPG (Hurwitz et al. 1999; Jing and Weiss 2001; Rosen et al. 1991). In the pedal ganglion, a cluster of PRQFVa positive neurons near the pleuropedal connective corresponds to an area that has been reported to contain motor neurons that control movements of the neck, foot, body wall, and parapodia (Nagahama et al. 1993). All of these structures are involved in the appetitive phase of feeding behavior, but they also participate in other behaviors, e.g., defensive behaviors. Thus it is unlikely that PRQFVa positive neurons are involved solely in the control of feeding behaviors. The highest density of staining was observed in the abdominal ganglion. This ganglion controls a number of motor functions including control of the cardiovascular system. Importantly, the abdominal ganglion has been implicated in the control of cardiovascular responses during feeding (Dieringer et al. 1978; Koch et al. 1984; Koester and Koch 1987). In this context, it is important to note that the most pronounced peripheral PRQFVa staining that we observed is present in the vascular system. Notably, PRQFVa is present in a number of neurons that are not thought to be involved in feeding, e.g., the RUQ neurons (Frazier et al. 1967). Overall, the distribution of PRQFVa suggests that its actions are unlikely to be limited to structures that participate exclusively in the generation of feeding behavior, and indeed, as evidenced by the presence of PRQFVa immunoreactivity in the branchial nerve and the gill, this peptide may also be involved in the control of structures that do not participate in feeding (i.e., the gill).

Because of the extensive PRQFVa staining within the buccal neuropile, we examined the bioactivity of this peptide on the excitability of selected buccal neurons, B4/5, B8, and B31/32. PRQFVa reduced the excitability of B31/32 and B4/5 but did not affect B8 excitability. Thus PRQFVa is not a general suppressor of neuronal excitability. The fact that PRQFVa is present in buccal ganglia and modulates the excitability of at least some buccal neurons supports the hypothesis that this peptide is involved in the central control of feeding behavior. Interestingly, it is known that B4/5 is strongly active in egestive motor programs and is less active in ingestive motor programs (Church and Lloyd 1994; Jing and Weiss 2001). Thus the suppressive action of PRQFVa on B4/5 excitability may contribute to the generation of ingestive motor programs. The presence of PRQFVa immunoreactivity in buccal neurons raises the possibility that peptides localized to neurons that are intrinsic to buccal ganglia may be in part the source of modulation that PRQFVa exerts on buccal ganglia. In this context, it is interesting to mention the asymmetrical neuron that is PRQFVa positive. Asymmetrical neurons are extremely rare in buccal ganglia. The PRQFVa positive buccal neuron is located in a position that is similar to the asymmetrical slow oscillator (SO) neuron that was described in another mollusk, *Lymnaea* (Elliott and Benjamin 1985). While it is not known yet whether SO contains PRQFVa, the fact that SO is an important interneuron in the feeding circuit of *Lymnaea* raises the possibility that the asymmetrical PRQFVa immunopositive neuron in *Aplysia* may be an important interneuron as well.

Since PRQFVa was purified from CNS extracts, it was important to determine if the peptide was also present in the gut. For this, we used immunostaining with the antibody we had determined was specific for PRQFVa. We found PRQFVa positive processes throughout the gut, including processes associated with the musculature. Since PRQFVa was purified from CNS extracts based on suppression of gut contractions, we also sought to confirm that synthetic PRQFVa exerted the same actions as the native peptide. We found that the synthetic peptide suppressed the myogenic activity of the gut (IC_{50} = approximately 10^{-7}). The majority of the PRQFVa staining in the gut was associated with the vasculature. The dense staining of PRQFVa immunostained processes observed in the vasculature of the gut extended to the gastroesophageal artery, the artery that supplies the gut. In addition to the vasculature of the gut, the vasculature of the gill and the highly vascularized kidney also contained numerous PRQFVa immunopositive processes. Furthermore, the abdominal ganglion, which contains the majority of central neurons controlling the *Aplysia* cardiovascular system, had the most abundant expression of PRQFVa in the CNS. These observations suggested a likely role of PRQFVa in control of the vasculature. To determine if PRQFVa was bioactive on vasculature, we used a preparation of anterior aorta in which contractions could be induced by nerve stimulation. Consistent with these immunocytological observations, we found that PRQFVa was bioactive on the vasculature. PRQFVa suppressed contractions of the anterior aorta that were elicited by nerve stimulation. The concentration-response relationship of PRQFVa on contractions of the vasculature was similar to that of the gut, with an IC_{50} of 10^{-7} M. These results suggest that, in addition to suppressing contractions of the gut musculature, PRQFVa may suppress contractions of the gut vasculature. We do not know if PRQFVa suppresses contractions of all the vascular tissues, but given that the bioactivity of PRQFVa that we observed on both central and peripheral targets was uniformly inhibitory, it may be that this peptide typically acts as a suppressor of activity.

General

We have recently purified from *A.kurodai* tissue several other peptides that have –FVamide in their C-termini. Molecular cloning of their precursors in *A.californica* has revealed clearly that they are processed from the two distinct precursors (AMRPs and enterins) and therefore fall into two families (Fujisawa et al. 1999; Furukawa et al. 2001). The cloning of the PRQFVa precursor reveals a third family of –FV amide neuropeptides. This family has some notable differences. In the case of the other two families, the precursor encodes for other peptides that are not FVamides. AMRPs and enterins are also different in that they do not share another common feature of PRQFVa and its related peptides, namely no arginine is present on the –4. Also, in the –3 position, AMRPs and enterins do not have a glutamine or an acidic amino acid. However, despite these differences, neuropeptides in the three families share some features. All amidated peptides encoded by the precursors for enterins, AMRP, and PRQFVa have a hydrophobic residue at the –1 position and a phenyalanine at the –2 position. Interestingly, the peptides derived from all three precursors have similar physiological actions. Similar structural features (FXamide where X = hydrophobic amino acid) and bioactivity of peptides have been identified in other species of mollusks (e.g., Muneoka et al. 2000) and annelids (Ikeda et al. 1993; Ukena et al. 1996). Even in vertebrates, some of the opioid peptides (e.g., endomorphins) possess similar structural features and bioactivity (McConalogue et al. 1999; Storr et al. 2002; Zadina 2002).

In mammals, many neuropeptides have been implicated in the regulation of the feeding system (Strand 1999), and the same is true for *Aplysia*. PRQFVamide joins the growing list of peptides that are present in and act on the feeding system of *Aplysia*. Past work has characterized, to varying extents, the distribution and actions of various peptides within the feeding circuit and peripheral feeding organs. These neuropeptides alter the output of the feeding circuitry and peripheral machinery in a variety of ways. In the CNS, some neuropeptides, such as small cardioactive peptide (SCP) (Sossin et al. 1987) and feeding circuit activating peptide (FCAP) (Sweedler et al. 2002), activate rhythmic output of the normally quiescent feeding CPG. Other neuropeptides exert modulatory effects on the rhythmic output of the CPG once it has been activated. CP2 (Phares and Lloyd 1996) and cerebrin (Li et al. 2001), for example, both shorten the duty cycle feeding motor programs (Li et al. 2001; Morgan et al. 2000). Yet another peptide, APGW, alters the phase relationships of different elements in the feeding motor program (Jing and Weiss 2001; Morgan et al. 2002), thereby switching the type of feeding behavior elicited. In addition to their diverse actions on the central feeding circuitry, many neuropeptides exert effects in the periphery as well. Several neuropeptides localized to motor neurons have been shown to regulate the contraction amplitude and relaxation rate of those motor neurons' target muscles (Hurwitz et al. 2000; Weiss et al. 1992). In the gut, several neuropeptides have been shown to alter motility. For example, SCP can increase gut motility (Lloyd et al. 1988). In contrast, enterins (Furukawa et al. 2001), AMRPs (Fujisawa et al. 1999), and as shown in this study, PRQFVamide can decrease gut motility.

In many of these cases, the modulatory effects of the neuropeptides on the feeding motor programs are at least partially caused by the peptides altering the firing of specific elements of the feeding CPG. In some cases, neuropeptides have even been shown to mimic effects caused by the firing of certain neurons that contain them. For example, APGW, a neuropeptide that is present in CBI-3, mimics the ability of CBI-3 firing to convert egestive motor programs to ingestive motor programs (Jing and Weiss 2001; Morgan et al. 2002) and also mimics CBI-3's ability to selectively inhibit B4/5 and B20, neurons highly active during egestive programs (Jing and Weiss 2001). For other peptides, however, like the enterins (Furukawa et al. 2001) and PRQFVa, which have been shown to inhibit B4/5 as well, the neurons responsible for this action remained to be characterized.

Finally, the similarity of actions of PRQFVa, AMRPs, and enterins on the gut, as well as the similarity of actions of PRQFVa and enterins on B4/5, raises the issue of whether these peptides are redundant. The fact that these peptides originate from different neurons that may be active in different feeding behaviors makes it difficult to conclude that they are redundant. A good illustration of this point is provided by the study that compared the actions of several neurons containing overlapping sets of transmitters/modulators (Blitz et al. 1999). Our cautious view is also supported by the fact that peptides with identical action (Swensen and Marder 2000) may not be released at the same time or onto the same targets. Even if such peptides are released at the same time, depending on amounts released, these peptides may exert either additive actions or occlude each other. Additionally, previous history of the system may also affect peptide actions (Dickinson et al. 1997). It also has become clear that, when actions of peptides that exert qualitatively similar effects have been studied in more detail, the joint actions of such peptides often produce effects that cannot be elicited by any of these peptides acting alone (Brezina et al. 1996). The true biological significance of the use of multiple modulators within a system is only beginning to emerge (Brezina and Weiss 1997; Nusbaum et al. 2001) and clearly depends on the characterization of the full complement of neuropeptides that operate in the system.

The authors thank Dr. Gregg Nagle for the generous gift of the *Aplysia* cDNA library and Dr. Elizabeth Cropper for critical reading of this manuscript.

This work was supported by Grant-in-Aid 10440249 from the Ministry of Education, Science, Sports and Culture of Japan to O. Matsushima. Y. Furukawa was supported by the SUNBOR grant from the Suntory Institute for Bioorganic Research. *Aplysia californica* were partially provided by the National Resource for *Aplysia* at the University of Miami under National Institutes of Health (NIH) Grant RR-10294. The support of the NIH through Grants NS-31609 to J. V. Sweedler, MH-50235 and K05-MH-01427 to K. R. Weiss, and DA-13330 to F. S. Vilim is gratefully acknowledged.

REFERENCES

Blitz DM, Christie AE, Coleman MJ, Norris BJ, Marder E, and Nusbaum MP. Different proctolin neurons elicit distinct motor patterns from a multifunctional neuronal network. *J Neurosci* 19: 5449–5463, 1999.

Brezina V, Orekhova IV, and Weiss KR. Functional uncoupling of linked neurotransmitter effects by combinatorial convergence. *Science* 273: 806–810, 1996.

Brezina V and Weiss KR. Analyzing the functional consequences of transmitter complexity. *Trends Neurosci* 20: 538–543, 1997.

Chomczynski P and Sacchi N. Single-step method of RNA isolation by acid guanidinium thiocyanate- phenol-chloroform extraction. *Anal Biochem* 162: 156–159, 1987.

Church PJ and Lloyd PE. Activity of multiple identified motor neurons recorded intracellularly during evoked feedinglike motor programs in *Aplysia*. *J Neurophysiol* 72: 1794–1809, 1994.

Church PJ, Whim MD, and Lloyd PE. Modulation of neuromuscular transmission by conventional and peptide transmitters released from excitatory and inhibitory motor neurons in *Aplysia*. *J Neurosci* 13: 2790–2800, 1993.

Cropper EC, Lloyd PE, Reed W, Tenenbaum R, Kupfermann I, and Weiss KR. Multiple neuropeptides in cholinergic motor neurons of *Aplysia*: evidence for modulation intrinsic to the motor circuit. *Proc Natl Acad Sci USA* 84: 3486–3490, 1987a.

Cropper EC, Tenenbaum R, Kolks MA, Kupfermann I, and Weiss KR. Myomodulin: a bioactive neuropeptide present in an identified cholinergic buccal motor neuron of *Aplysia. Proc Natl Acad Sci USA* 84: 5483–5486, 1987b.

Dickinson PS, Fairfield WP, Hetling JR, and Hauptman J. Neurotransmitter interactions in the stomatogastric system of the spiny lobster: one peptide alters the response of a central pattern generator to a second peptide. *J Neurophysiol* 77: 599–610, 1997.

Dieringer N, Koester J, and Weiss KR. Adaptive changes in heart rate of *Aplysiacalifornica. J Comp Physiol A* 123: 11–21, 1978.

Eberwine James H, Valentino KL, and Barchas JD. *In Situ Hybridization in Neurobiology: Advances in Methodology.* New York: Oxford, 1994.

Eipper BA, Stoffers DA, and Mains RE. The biosynthesis of neuropeptides: peptide alpha-amidation. *Annu Rev Neurosci* 15: 57–85, 1992.

Elliott CJ and Benjamin PR. Interactions of the slow oscillator interneuron with feeding pattern- generating interneurons in *Lymnaea stagnalis*. *J Neurophysiol* 54: 1412–1421, 1985.

Frazier WT, Kandel ER, Kupfermann I, Waziri R, and Coggeshall RE. Morphological and functional properties of identified neurons in the abdominal ganglion of *Aplysia californica*. *J Neurophysiol* 30: 1288–1351, 1967.

Fujisawa Y, Furukawa Y, Ohta S, Ellis TA, Dembrow NC, Li L, Floyd PD, Sweedler JV, Minakata H, Nakamaru K, Morishita F, Matsushima O, Weiss KR, and Vilim FS. The *Aplysiamytilus* inhibitory peptide-related peptides: identification, cloning, processing, distribution, and action. *J Neurosci* 19: 9618–9634, 1999.

Furukawa Y, Nakamaru K, Wakayama H, Fujisawa Y, Minakata H, Ohta S, Morishita F, Matsushima O, Li L, Romanova E, Sweedler JV, Park JH, Romero A, Cropper EC, Dembrow NC, Jing J, Weiss KR, and Vilim FS. The enterins: a novel family of neuropeptides isolated from the enteric nervous system and CNS of *Aplysia*. *J Neurosci* 21: 8247–8261, 2001.

Hurwitz I, Cropper EC, Vilim FS, Alexeeva V, Susswein AJ, Kupfermann I, and Weiss KR. Serotonergic and peptidergic modulation of the buccal mass protractor muscle (I2) in *Aplysia. J Neurophysiol* 84: 2810–2820, 2000.

Hurwitz I, Perrins R, Xin Y, Weiss KR, and Kupfermann I. C-PR neuron of *Aplysia* has differential effects on "Feeding" cerebral interneurons, including myomodulin-positive CBI-12. *J Neurophysiol* 81: 521–534, 1999.

Ikeda T, Kubota I, Miki W, Nose T, Takao T, Shimonishi Y, and Muneoka Y. Structures and actions of 20 novel neuropeptides isolated from the ventral nerve cords of an echiuroid worm, *Urechis unicinctus*. In: *Peptide Chemistry*, edited by Yanaihara N. Osaka, Japan: ESCOM, 1993, p. 583–585.

Jahan-Parwar B and Fredman SM. Cerebral ganglion of *Aplysia*: cellular organization and origin of nerves. *Comp Biochem Physiol A* 54: 347–357, 1976.

Jahan-Parwar B, Wilson AH Jr, and Fredman SM. Role of proprioceptive reflexes in control of feeding muscles of *Aplysia*. *J Neurophysiol* 49: 1469–1480, 1983.

Jing J and Weiss KR. Neural mechanisms of motor program switching in *Aplysia*. *J Neurosci* 21: 7349–7362, 2001.

Koch UT, Koester J, and Weiss KR. Neuronal mediation of cardiovascular effects of food arousal in *Aplysia*. *J Neurophysiol* 51: 126–135, 1984.

Koester J and Koch UT. Neural control of the circulatory system of *Aplysia*. *Experientia* 43: 972–980, 1987.

Kupfermann I. Functional studies of cotransmission. *Physiol Rev* 71: 683–732, 1991.

Li L, Floyd PD, Rubakhin SS, Romanova EV, Jing J, Alexeeva VY, Dembrow NC, Weiss KR, Vilim FS, and Sweedler JV. Cerebrin prohormone processing, distribution and action in *Aplysia* californica. *J Neurochem* 77: 1569–1580, 2001.

Lloyd PE, Kupfermann I, and Weiss KR. Evidence for parallel actions of a molluscan neuropeptide and serotonin in mediating arousal in *Aplysia*. *Proc Natl Acad Sci USA* 81: 2934–2937, 1984.

Lloyd PE, Kupfermann I, and Weiss KR. Central peptidergic neurons regulate gut motility in *Aplysia*. *J Neurophysiol* 59: 1613–1626, 1988.

Marder E, Christie AE, and Kilman VL. Functional organization of cotransmission systems: lessons from small nervous systems. *Invert Neurosci* 1: 105–112, 1995.

McConalogue K, Grady EF, Minnis J, Balestra B, Tonini M, Brecha NC, Bunnett NW, and Sternini C. Activation and internalization of the mu-opioid receptor by the newly discovered endogenous agonists, endomorphin-1 and endomorphin-2. *Neuroscience* 90: 1051–1059, 1999.

Morgan PT, Jing J, Vilim FS, and Weiss KR. Interneuronal and peptidergic control of motor pattern switching in *Aplysia. J Neurophysiol* 87: 49–61, 2002.

Morgan PT, Perrins R, Lloyd PE, and Weiss KR. Intrinsic and extrinsic modulation of a single central pattern generating circuit. *J Neurophysiol* 84: 1186–1193, 2000.

Morishita F, Sasaki K, Kanemaru K, Nakanishi Y, Matsushima O, and Furukawa Y. NdWFamide: a novel excitatory peptide involved in cardiovascular regulation of *Aplysia*. *Peptides* 22: 183–189, 2001.

Morton DW and Chiel HJ. The timing of activity in motor neurons that produce radula movements distinguishes ingestion from rejection in *Aplysia. J Comp Physiol* 173: 519–536, 1993.

Muneoka Y, Morishita F, Furukawa Y, Matsushima O, Kobayashi M, Ohtani M, Takahashi T, Iwakoshi E, Fujisawa Y, and Minakata H. Comparative aspects of invertebrate neuropeptides. *Acta Biol Hung* 51: 111–132, 2000.

Nagahama T, Weiss KR, and Kupfermann I. Effects of cerebral neuron C-PR on body postural muscles associated with a food-induced arousal state in *Aplysia. J Neurophysiol* 70: 1231–1243, 1993.

Nielsen H, Engelbrecht J, Brunak S, and von Heijne G. Identification of prokaryotic and eukaryotic signal peptides and prediction of their cleavage sites. *Protein Eng* 10: 1–6, 1997.

Nusbaum MP, Blitz DM, Swensen AM, Wood D, and Marder E. The roles of co-transmission in neural network modulation. *Trends Neurosci* 24: 146–154, 2001.

Phares GA and Lloyd PE. Immunocytological and biochemical localization and biological activity of the newly sequenced cerebral peptide 2 in *Aplysia*. *J Neurosci* 16: 7841–7852, 1996.

Rosen SC, Teyke T, Miller MW, Weiss KR, and Kupfermann I. Identification and characterization of cerebral-to-buccal interneurons implicated in the control of motor programs associated with feeding in *Aplysia*. *J Neurosci* 11: 3630–3655, 1991.

Sambrook J, Fritsch EF, and Maniatis T. *Molecular Cloning: A Laboratory Manual.* New York: Cold Springs Harbor Laboratory, 1989.

Sawada M, Blankenship JE, and McAdoo DJ. Neural control of a molluscan blood vessel, anterior aorta of *Aplysia*. *J Neurophysiol* 46: 967–986, 1981.

Seidah NG and Chretien M. Proprotein and prohormone convertases: a family of subtilases generating diverse bioactive polypeptides. *Brain Res* 848: 45–62, 1999.

Sossin WS, Kirk MD, and Scheller RH. Peptidergic modulation of neuronal circuitry controlling feeding in *Aplysia*. *J Neurosci* 7: 671–681, 1987.

Storr M, Hahn A, Gaffal E, Saur D, and Allescher HD. Effects of endomorphin-1 and -2 on mu-opioid receptors in myenteric neurons and in the peristaltic reflex in rat small intestine. *Clin Exp Pharmacol Physiol* 29: 428–434, 2002.

Strand FL. *Neuropeptides: Regulators of Physiological Processes.* Cambridge, MA: MIT Press, 1999.

Susswein AJ and Byrne JH. Identification and characterization of neurons initiating patterned neural activity in the buccal ganglia of *Aplysia*. *J Neurosci* 8: 2049–2061, 1988.

Sweedler JV, Li L, Rubakhin SS, Alexeeva V, Dembrow NC, Dowling O, Jing J, Weiss KR, and Vilim FS. Identification and characterization of the feeding circuit-activating peptides, a novel neuropeptide family of *Aplysia*. *J Neurosci* 22: 7797–7808, 2002.

Swensen AM and Marder E. Multiple peptides converge to activate the same voltage-dependent current in a central pattern-generating circuit. *J Neurosci* 20: 6752–6759, 2000.

Ukena K, Oumi T, Matsushima O, Takahashi T, Muneoka Y, Fujita T, Minakata H, and Nomoto K. Inhibitory pentapeptides isolated from the gut of the earthworm, *Eisenia foetida. Comp Biochem Physiol A* 114: 245–249, 1996.

Vilim FS, Alexeeva V, Moroz LL, Li L, Moroz TP, Sweedler JV, and Weiss KR. Cloning, expression and processing of the CP2 neuropeptide precursor of *Aplysia*. *Peptides* 22: 2027–2038, 2001.

Vilim FS, Price DA, Lesser W, Kupfermann I, and Weiss KR. Costorage and corelease of modulatory peptide cotransmitters with partially antagonistic actions on the accessory radula closer muscle of *Aplysia* californica. *J Neurosci* 16: 8092–8104, 1996.

Weiss KR, Brezina V, Cropper EC, Hooper SL, Miller MW, Probst WC, Vilim FS, and Kupfermann I. Peptidergic co-transmission in *Aplysia*—functional implications for rhythmic behaviors. *Experientia* 48: 456–463, 1992.

Zadina JE. Isolation and distribution of endomorphins in the central nervous system. *Jpn J Pharmacol* 89: 203–208, 2002.